ARTICLE

Self-Diffusion of Water and Simple Alcohols in Single-Walled Aluminosilicate Nanotubes

Ji Zang, Suchitra Konduri, Sankar Nair, and David S. Sholl*

School of Chemical & Biomolecular Engineering, Georgia Institute of Technology, 311 Ferst Drive NW, Atlanta, Georgia 30332-0100

ABSTRACT Understanding transport phenomena of fluids through nanotubes (NTs) is of great interest in order to enable potential application of NTs as separation devices, encapsulation media for molecule storage and delivery, and sensors. Single-walled metal oxide NTs are interesting materials because they present a well-defined solid-state structure, precisely tunable diameter and length, as well as a hydrophilic and functionalizable interior for tuning transport and adsorption selectivity. Here, we study the transport properties of hydrogen-bonding liquids (water, methanol, and ethanol) through a single-walled aluminosilicate NT to investigate the influence of liquid—surface and liquid—liquid interactions and the effects of competitive transport of different chemical species using molecular dynamics (MD) simulations. The self-diffusivities (D_s) for all the three species decrease with increasing loading and are comparable to bulk liquid diffusivities at low molecular loadings. We show that the hydrogen-bond network associated with water makes its diffusion behavior different from methanol and ethanol. Mixtures of water and methanol show segregation in the NT, with water located closer to the tube wall and the alcohol molecules localized near the center of the NT. D_s values of water in an analogous aluminogermanate NT are larger than those in the aluminosilicate NT due to a larger pore diameter.

KEYWORDS: inorganic nanotubes · aluminosilicate · self-diffusion · water · methanol · ethanol

Nanotubes (NTs) made from metal oxide such as aluminosilicate/germanate NTs are attracting increasing attention[1−6] because they can be synthesized with tunable composition and functionality *via* low-temperature liquid-phase chemistry using inexpensive precursors.[7,8] Unlike carbon NTs, both the diameters and lengths of synthetic aluminosilicate/germanate NTs are monodisperse,[7,8] a property that may be useful in a variety of applications. The diameter and length of these single-walled NTs can be controlled precisely and reproducibly by changing the Ge substitution ratio.[9] Using this approach, outer diameters and tube lengths varying from 2.2 to 3.3 nm and 100 to 15 nm, respectively, can be made. The NTs have a highly ordered wall structure with isolated silanol/germanol groups bound on the inner wall. The presence of hydroxyl groups on this inner wall makes the interior of the pore at least partially hydrophilic. These properties make them attractive candidates for a variety of potential applications, including molecular separations, molecular encapsulation, and sensors. The rates and mechanisms of molecular transport in the NTs are crucial to the development of these applications, but unlike the situation for carbon NTs,[10−17] little is currently known about molecular transport in aluminosilicate/germanate NTs.

A recent study examined diffusion and adsorption of water in aluminosilicate NTs using molecular dynamics (MD) simulations, grand canonical Monte Carlo (GCMC) simulations, and experimental sorption measurements.[18] This preliminary work confirmed the feasibility of obtaining high water transport rates through the NT, due to a combination of several factors—short NT length, hydrophilicity, and pore structure. Here, we extend this previous work in several directions using MD simulations of aluminosilicate and aluminogermanate NTs. First, we elucidate the transport mechanism of water in the NTs and examine diffusion of two other hydrogen-bonding liquids, methanol and ethanol. Diffusion in binary mixtures of these liquids is also investigated. These simulations provide a fundamental understanding of transport of fluids in single-walled metal oxide NTs and insights into potential applications of these materials in biofuel purification. Finally, we examine the diffusion of water in an aluminogermanate NT. Comparison of the diffusive properties of water in aluminosilicate and aluminogermanate NTs indicates how strongly the chemical variation in the NT structure affects molecular transport in these highly ordered nanopores.

*Address correspondence to david.sholl@chbe.gatech.edu.

Received for review February 23, 2009 and accepted April 27, 2009.

Published online May 8, 2009.
10.1021/nn9001837 CCC: $40.75

RESULTS AND DISCUSSION

Experimentally, it has been found that a range of single-walled aluminosilicogermanate NTs—from the aluminosilicate NTs with 12 gibbsite units in the circumference to aluminogermanate NTs with 18 units—can be synthesized by varying the Si/Ge ratio in the precursor solution. This diameter tunability has been explained by analyzing the internal energy of each structure as a function of pore diameter.[9,19,20] Our simulations used the aluminosilicate and aluminogermanate end members of the NT series, as shown in Figure 1.

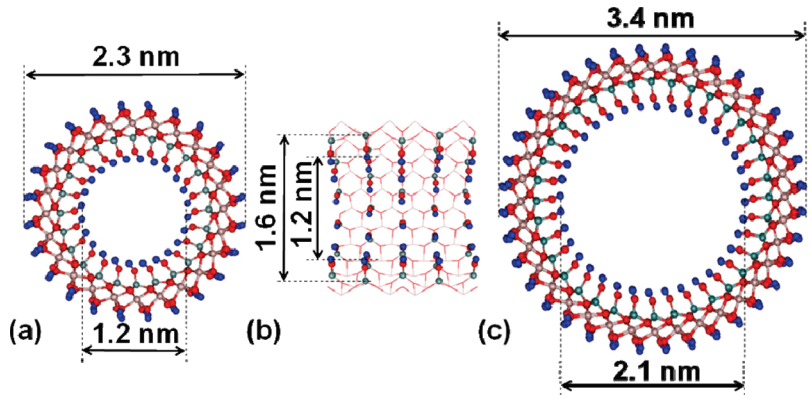

Figure 1. (a) Atomic structure of aluminosilicate NT viewed along the axial direction. (b) Side view of aluminosilicate NT shell showing the tube interior with the silanol groups inside the pore shown in ball and stick format. The hydroxyl groups on the outer surface of the NT are not shown for clarity. (c) Similar to (a) but for an aluminogermanate NT. Blue, hydrogen; red, oxygen; pink, aluminum; gray, silicon in (a) and (b) and germanium in (c).

In this section, we will first discuss the general trends in self-diffusivities as a function of the density of single-component molecules inside aluminosilicate NTs. Then, we explore the transport mechanism of isolated water molecules in the aluminosilicate NT to explain the diffusion behavior of molecules at low loadings. To understand water diffusion at high loadings, our MD results are examined in terms of hydrogen bonding in the diffusing molecules. After comparing D_s of all three liquids and discussing those of molecules in binary mixtures in aluminosilicate NTs, we compare the diffusion of water in aluminosilicate and aluminogermanate NTs.

Diffusion of Single-Component Water, Methanol, and Ethanol in Aluminosilicate NTs. Figure 2 shows the room temperature self-diffusivity from MD simulations of single-component water, methanol, and ethanol for a wide range of pore loadings in the aluminosilicate NT shown in Figure 1. Unlike carbon NTs, aluminosilicate/germanate NTs have a corrugated inner surface with periodic wider and narrower regions due to the presence of hydroxyl groups, as shown in Figure 1b. Because of this pore structure, it is not possible to unambiguously define the total pore volume available to molecules in the NTs. We used the average of the diameters of these two regions (the largest H to H and Si to Si distances in planes perpendicular to the tube axis as the diameter of the narrow and wide region) to calculate the total pore volume and hence the loading. A related quantity that can be unambiguously defined is the one-dimensional molecular density. For water, methanol, and ethanol, a density of 0.1 g/cm^3 as used in Figure 2 corresponds to a one-dimensional density of 5.15, 2.89, and 2.01 molecules/nm along the pore axis, respectively. For comparison, D_s values for bulk water, methanol, and ethanol at 298 K are shown as horizontal lines in Figure 2. These diffusivities were calculated from NVT-MD simulations with the densities fixed at their experimental values.

The self-diffusivity of all three species decreases with increasing pore loading, with methanol and ethanol showing stronger decreases at higher loadings than water. For all three species, D_s at low loadings is larger than in the bulk liquid state, while the opposite is true at high loadings. In very general terms, there is not much spatial confinement for molecules at low loadings except the interaction between the molecule and NT, while at high loadings there is less space for individual molecules to diffuse. The liquid−surface interaction is an additional factor that will alter the diffusion compared with bulk phase. In the case of water diffusion in aluminosilicate NTs, our results agree with the results presented previously by Konduri *et al.*[18] To our best knowledge, no similar simulations have been done before for methanol and ethanol. Below, we will examine the water diffusion mechanism in detail to characterize the diffusion of hydrogen-bonding liquids in aluminosilicate NTs as the pore loading is varied.

Diffusion of Isolated Water Molecules in Aluminosilicate NT. One initial way to characterize the molecules inside the aluminosilicate NTs is *via* the radial distributions of the molecules' O atoms. The observed distributions for water at several different loadings and methanol and ethanol at low loadings are shown in Figure 3. Each calculated value in these distributions corresponds to the probability of finding a molecule in a cylinder of radial thickness 0.1 Å. For isolated water molecules (density 0.012 g/cm^3 in Figure 3), molecules are observed in the range of 4−6.2 Å

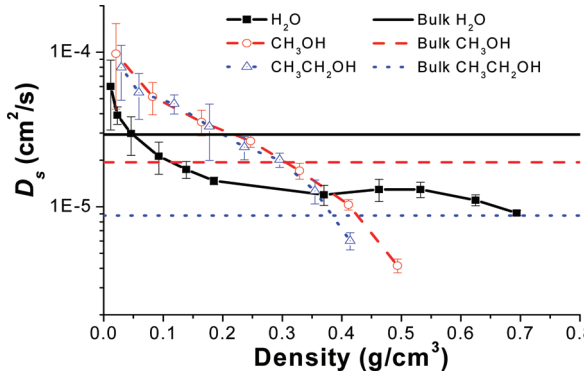

Figure 2. Self-diffusivities of water, methanol, and ethanol as a function of loading in aluminosilicate NT. The self-diffusivities for bulk water, methanol, and ethanol are also shown.

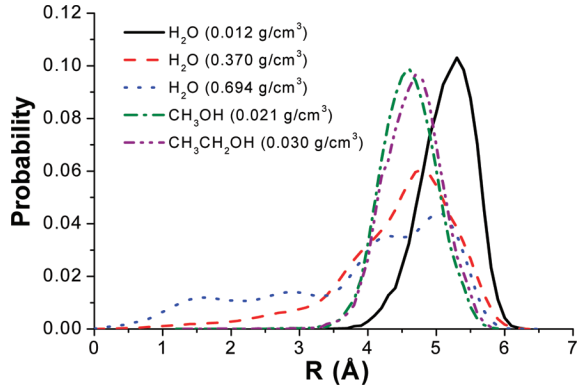

Figure 3. Probability of finding water, ethanol, and methanol in the radial direction of aluminosilicate NT.

(from the NT axis) in the radial direction. It is helpful in examining Figure 3 to note from Figure 1 that the radial coordinate of the inner H atoms on the pore surface is approximately 6 Å. The radial distributions of methanol and ethanol at low loadings are very similar to one another, with molecules located almost exclusively in the range of 3.7−5.7 Å. These distributions indicate that all liquid molecules diffuse along/near the tube wall at low loadings. The stable positions for water in the aluminosilicate NT are closer to the tube wall than methanol and ethanol. The distribution of water at higher loadings will be discussed later.

To give insight into the transport of hydrogen-bonding liquids in aluminosilicate NTs, it is helpful to examine the transport mechanism of water in the NT at dilute loading. To describe the potential energy surface of an isolated water molecule in the NT, we generated a grid inside the NT with intervals of 0.1 Å in the axial and radial directions and 1° in the circumferential direction. At each grid point, we fixed the water oxygen and placed two hydrogen atoms with 1 Å H−O bond lengths and 109.47° H−O−H angle, at 100−1000 randomly selected orientations. For each orientation, the H atoms and all atoms in the NT were then allowed to relax to a local energy minimum (while holding the O atom constrained at the grid point). This procedure gives an accurate estimate for the minimum energy available to a water molecule inside the NT as a function of the water molecule's O atom position.

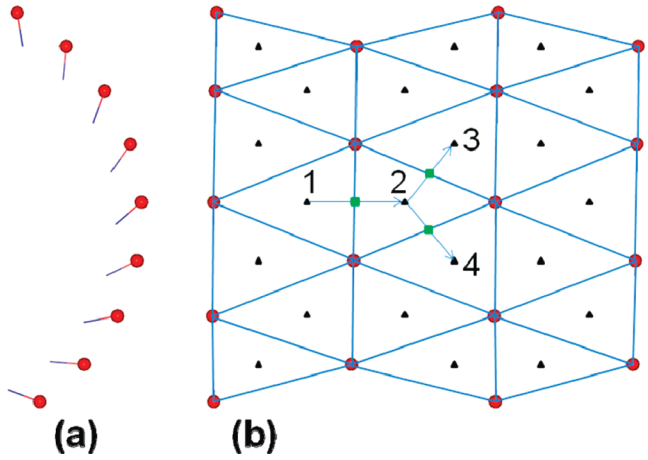

Figure 4. (a) Partial cross section of aluminosilicate NT, showing only the inner surface hydroxyl groups. Red circles are oxygen atoms. (b) Side view of (a) showing only the O atoms. Black triangles are energy minima where a water forms three hydrogen bonds with the inner surface, and green squares are the transition state positions where only two hydrogen bonds can be formed.

Figure 4 illustrates the resulting potential energy surface for a single water molecule along the tube axis. The most stable positions for water molecules lie in triangles defined by three neighboring oxygen atoms in the pore wall (marked as triangles in Figure 4b). In these positions, water forms three hydrogen bonds with the tube's inner surface. The radial position of these minimum energy states is about 5.6 Å, which is close to the peak of the radial distribution of the isolated water molecule shown in Figure 3. We used a simple criterion to define hydrogen bonds by considering water molecules and the pore wall to form a hydrogen bond if the oxygen−oxygen distance is less than 3.7 Å.[21] The minimum energy path between adjacent minima follows the paths shown as 1−2, 2−3, or 2−4 in Figure 4b. At the transition state (marked as squares in Figure 4b) along these paths, the water molecule forms two hydrogen bonds with the inner surface. In the radial direction, the energy minima are closer to the tube wall than the transition states. The energy barrier defined by the transition states separating adjacent minima is 0.18 eV (17.4 kJ/mol).

We also carried out MD simulations of individual water molecules diffusing in the aluminosilicate NT at temperatures from 298 to 600 K. Fitting the observed values of D_s with an Arrhenius equation gave an activation energy of 0.10 eV. This activation energy is only about half of the energy barrier mentioned above, strongly suggesting that a straightforward application of transition state theory (TST) cannot describe water motion in this system. To understand this observation, it is important to note that the orientation of the water molecule plays a critical role in determining water−nanotube interactions. Even when the water's oxygen atom is fixed, many metastable configurations with energies higher than the minimum energy for the grid point typically exist. Loosely speaking, some orientations of the molecule see the NT as "stickier" than others.

The implications of this situation can be seen from the representative trajectory shown in Figure 5, which shows 1 ns of dynamics for a single water molecule diffusing at 298 K. The displacement of water in the axial coordinate is shown in units of half the unit cell length, which is the distance between two neighboring planes of hydroxyl groups perpendicular to tube axis. With these units, a hopping event between energy minima located along the axial direction occurs when the displacement changes by ±1. If a simplistic application of TST was valid, mobility of water would occur by an uncorrelated series of hops of length ±1 along the pore axis. It is evident from Figure 5 that motion does not oc-

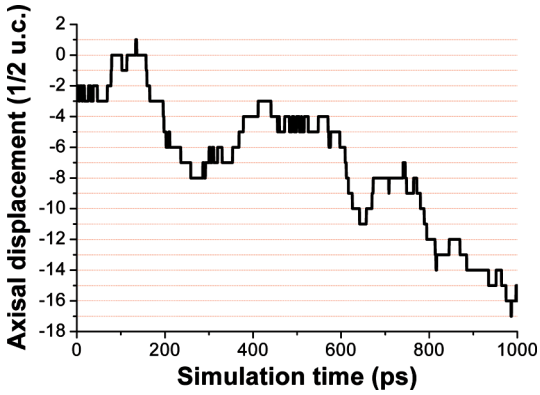

Figure 5. Trajectory of an isolated water molecule in an aluminosilicate NT at 298 K. Displacement in the axial direction is in units of half the unit cell length.

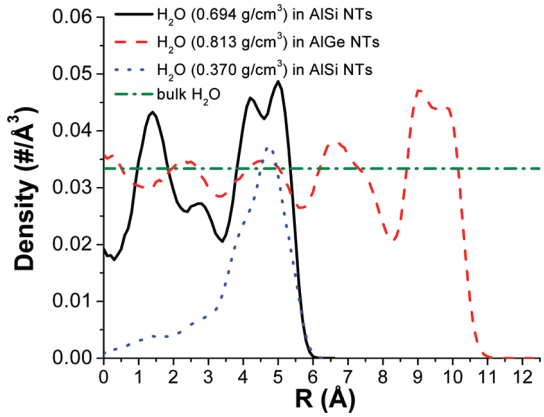

Figure 6. Density profile of water in aluminosilicate and aluminogermanate NTs compared with bulk water. The NT pore was divided in the same way as in Figure 3 to calculate the density.

cur in this way; there are several sections of the trajectory where the molecule moves through multiple energy minima in a correlated way.

To analyze these one-dimensional motions quantitatively, we defined the end of a hop to occur when the molecule spends longer than 4 ps within an individual half unit cell mentioned above. Our conclusions were not sensitive to the precise time interval chosen for this purpose.[22] In the trajectory shown in Figure 5, there are 50 hops that jumped half a unit cell and 6 hops that jumped 1 unit cell in the axial direction. We performed a similar analysis for an 8 ns trajectory at 298, 400, 500, and 600 K, and the resulting hop length distributions are shown in Table 1. With increasing temperature, more hops spanning multiple local minima were observed. At 500 K, for example, we observed hops covering as many as 4 unit cells. From the discussion above, it can be seen that a water molecule needs to have an appropriate orientation relative to the tube wall in order to be captured by the energy minima. The extended hops that become more prevalent at higher temperatures are associated with molecules that lose this preferential alignment and then interact more weakly with the pore wall, allowing them to move extended distances along the pore axis.

From the hop length distributions, we can estimate D_s *via* the relation $\sum_n (nL/2)^2 N_n = 2D_s t$, where L and t are, respectively, the unit cell length in the axial direction and the total simulation time of a trajectory. This expression will correctly describe the net diffusivity if the hops described by the hop length distribution are uncorrelated.[23] Listed as D_{hop} in Table 1, the diffusivities estimated in this way agree with those calculated directly from our MD simulations (D_{MD} in Table 1), indicating that a description of the dynamics of molecules in the dilute loading limit in terms of the hop length is sufficient to characterize this system.

Diffusion of Water in Aluminosilicate NT at Nondilute Loadings. Now we return to Figure 3 and discuss the radial distributions of water at nondilute pore loadings. As the water density increases from 0.012 to 0.694 g/cm^3, molecules first occupy the region near the pore wall and then gradually fill locations closer to the tube axis. At the highest pore loading shown in Figure 3, there is a significant increase in the fraction of water in the range of 1−3.5 Å in the radial direction compared with lower pore loadings. An alternative way to view the distribution of water molecules is shown in Figure 6 for pore loadings of 0.370 and 0.694 g/cm^3. In Figure 6, the local water density is shown in units of molecules/Å^3, with the density of bulk water shown for comparison. It can be seen from these data that there is one layer of water molecules located close to the tube wall at a loading of 0.370 g/cm^3, while at 0.694 g/cm^3 loading, a second layer of water molecules also exists nearer to the tube axis.

It is also useful to characterize the hydrogen bonding between water molecules during diffusion in aluminosilicate NTs. We used the definition of hydrogen bonds mentioned above in which the O−H−O angle was not considered. Using more strict conditions to define the number of hydrogen bonds[24] will give smaller number of hydrogen bonds than are listed below. In our simulations with a pore loading of 0.046 g/cm^3 in an aluminosilicate NT, only four distinct water molecules are present in our simulation volume. For each molecule, more than half (57.9%) of the total diffusion time is spent hydrogen-bonded to at least one other water molecule. This observation implies that water readily forms clusters at low loadings in

TABLE 1. Hop Length Distributions and D_s Calculated for Isolated Water Molecules in Aluminosilicate NT as Temperature is Varied[a]

	N_n for n = 1−12													
T (K)	1	2	3	4	5	6	7	8	9	10	11	12	D_{MD} (cm^2/s)	D_{hop} (cm^2/s)
298	353	25	1	1	0	0	0	0	0	0	0	0	6.02×10^{-5}	5.46×10^{-5}
400	440	108	24	7	1	1	0	0	0	0	0	0	1.60×10^{-4}	1.44×10^{-4}
500	296	110	43	18	6	4	5	1	0	0	0	0	2.50×10^{-4}	2.30×10^{-4}
600	222	106	65	45	18	17	13	2	2	1	0	1	4.10×10^{-4}	4.78×10^{-4}

[a] Values of n and N_n are the hop lengths in units of half the unit cell length and the number of hops that jumped length n, respectively. D_{MD} is calculated directly from our MD trajectories, while D_{hop} is from the analysis of hop length distributions described in the text.

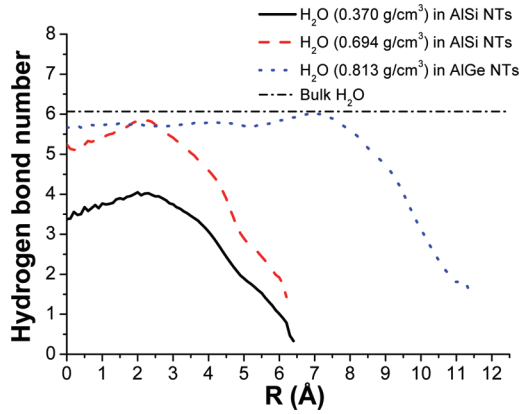

Figure 7. Number of hydrogen bonds formed per water molecule with other water molecules as a function of the water's radial position in aluminosilicate and aluminogermanate NTs.

the pore, and this clustering is in large part the origin of the reduction in the observed diffusivity with density at low loadings. This clustering effect has been observed to play an important role in diffusion of water at low loadings in carbon NTs.[25] At high loadings, the water diffusion behavior is quite different. Unlike methanol and ethanol, D_s for water does not decrease significantly as pore density is increased beyond 0.2 g/cm^3. This is due to the contribution from fast diffusion of water molecules located further from the tube wall. In Figure 7, the number of hydrogen bonds per water molecule with other water molecules (not with the pore wall) as a function of the molecule's radial position at different pore loadings is shown. The result for bulk water is also shown for comparison. At the highest loading shown in Figure 7, the water in the inner layer in the pore has a similar local environment to water in bulk phase. It is not surprising, therefore, that the diffusion of water in the pore at these loadings is quite similar to the diffusion that occurs in bulk water.

Self-diffusivities of water in other NTs such as carbon NTs[26−29] and boron nitride NTs[30] have been studied previously with experiments and MD simulations. The diffusivities reported in these materials vary by 3 orders of magnitude, from 10^{-5} to 10^{-2} cm^2/s, with different water loadings and the size and chemical functionality of NTs. Striolo[29] studied the effect of the presence of isolated oxygenated sites in carbon NTs on transport properties of confined water and concluded that these sites significantly decrease the diffusion coefficient of water relative to the result in pristine NTs. Striolo's calculations predicted a diffusivity of $\sim 10^{-5}$ cm^2/s in an (8,8) nanotube that includes oxygenated sites. This diffusivity is 2−3 orders of magnitude smaller than for pristine NTs of similar size at low water loadings. The diffusivities observed in our calculations for AlSi nanotubes are similar in magnitude to the results just mentioned for partially oxygenated carbon NTs. Compared with diffusion of water in zeolites (in the order of 10^{-6}−10^{-8} cm^2/s),[31] water diffuses more rapidly in aluminosilicate NTs. This is due to both the larger pore diameter of the present NT and the absence of metal cations that strongly interact with water.[18]

Comparison between Diffusion of Different Liquids in the Aluminosilicate NT. For applications of the NTs in liquid-phase separations, it will be helpful to know the difference among D_s for different chemical species. The self-diffusivities of pure water, methanol, and ethanol in aluminosilicate NTs at 298 K are compared in Figure 2. The diffusivities of methanol and ethanol are larger than those of water at low loadings because water is more restricted by water−NT and water−water interactions in terms of hydrogen bonding. The radial distributions of methanol and ethanol in the pore at low loading are shown in Figure 3. The average oxygen radial positions for methanol and ethanol are 4.65 and 4.70 Å, respectively; this is considerably further from the tube wall compared with the equivalent quantity for water (5.21 Å). It is not surprising that water interacts more strongly with the pore wall than the alcohols since a water molecule can form more hydrogen bonds with the wall than either alcohol. The weaker interactions between tube wall and alcohols and between alcohols make the decrease of diffusivities for alcohols with increasing loading density slower than water. As a result, D_s for the alcohols is not reduced below the bulk phase values until relatively high loadings are achieved. The diffusivities of methanol and ethanol are similar except at high loadings. At the highest loadings we examined, ethanol diffuses more slowly than methanol. At pore loadings larger than ~0.40 g/cm^3, water has higher diffusivities than either of the alcohols. At a pore loading of 0.5 g/cm^3, for example, the diffusivity of pure water is about four times larger than the diffusivity of pure methanol.

All of the simulations above examined diffusion of single-component liquids. To examine the diffusion of simple water/alcohol mixtures in aluminosilicate NTs, we first calculated D_s for water/methanol mixtures with different molar compositions. These results are shown in Figure 8. In these NVT-MD simulations, the number of molecules was determined so that the mixture densities are those of ideal bulk mixtures calculated from experimental values for the single-component densities at room temperature. The addition of even relatively small amounts of methanol to the mixture strongly reduces the diffusivity of water. With increasing methanol content, D_s for water continues to decrease. Methanol diffusion also decreases with increasing water content.

Figure 9 shows the computed diffusion coefficients of water and methanol in equimolar mixtures inside aluminosilicate NTs. Here, the density used to indicate the results for water or methanol in the mixture is the total density of the mixture. The observed diffusivities for pure water and methanol in the NT are also shown in the same figure. When the density of the mixture is described as just defined, the observed diffusivities for water and methanol in the mixture are not very different from the pure component results. At high pore loadings, D_s for

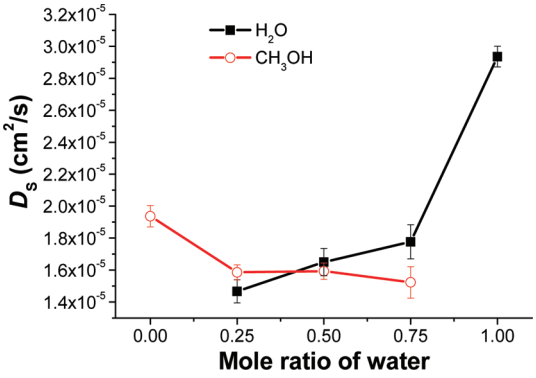

Figure 8. Self-diffusivities of molecules in bulk mixtures of water and methanol.

water in the mixture keeps decreasing as the loading is increased, unlike the case for pure water in the NT. As we already observed in bulk mixtures, methanol slows diffusion of water. We have also performed similar calculations for mixtures inside the NT with 3:1 and 1:3 molar compositions. The details of these calculations are shown in Supporting Information Figure 1. In general, our description of the results for the equimolar mixture also applies to these other molar compositions.

Representative radial distributions of water and methanol in equimolar mixtures and as pure components inside aluminosilicate NTs are shown in Figure 10. In this figure, the pure component data come from simulations of water (methanol) with a loading of 0.185 g/cm^3 (0.329 g/cm^3), while the mixture data are from simulations with a total density of 0.514 g/cm^3. In the mixture, the peak for water is closer to the tube wall than for water as a pure component. For methanol, the effect is the opposite: methanol is closer to the wall in a pure component than in the mixture. Similar effects were observed for water and ethanol mixtures.

To study the effect of alcohol chain length on diffusion of water/alcohol mixtures, simulations of water and ethanol diffusion in equimolar composition in an aluminosilicate NT were performed. The observed diffusivities

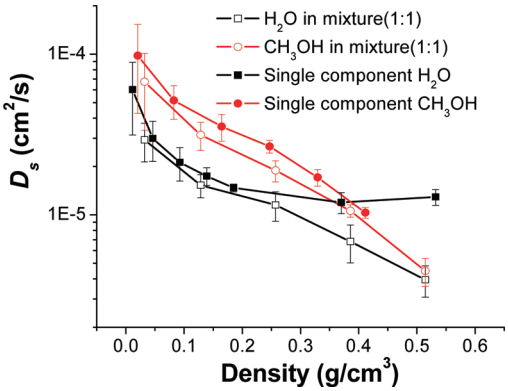

Figure 9. Self-diffusivities of molecules in 1:1 water and methanol mixtures (unfilled symbols) in aluminosilicate NT. Results for water and methanol as pure components inside the NT are also shown (filled symbols).

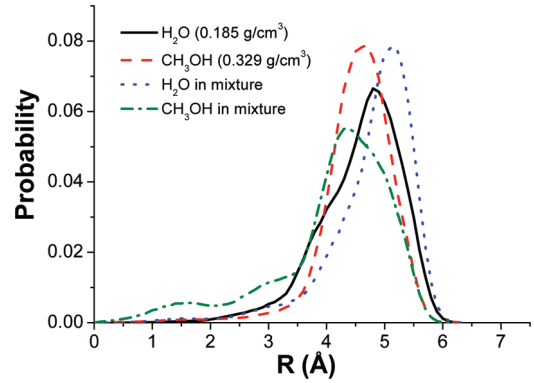

Figure 10. Radial distribution of liquids in an aluminosilicate NT for the conditions described in the text. The NT pore was divided in the same way as in Figure 3.

are shown in Figure 11. The trends in these results are very similar to the water/methanol mixtures discussed above. For completeness, we also studied diffusion of methanol and ethanol in equimolar mixtures in the NT. As can be seen from Figure 12, there are not strong differences between the observed self-diffusivities for these mixtures and the pure components.

Diffusion of Water in Aluminogermanate NTs. To understand how strongly the substitution of Si with Ge in the NTs and the diameter of NTs affects molecular transport in the NTs, we studied D_s of water in the aluminogermanate NT shown in Figure 1. The self-diffusivities from these calculations are shown in Figure 13. The dependence of the diffusivity of water on loading is similar to that observed in the aluminosilicate NT, although D_s for water in the aluminogermanate NT is higher. The main reason for the faster diffusion in the aluminogermanate NT at nondilute pore loadings is the larger pore space available in this NT relative to the aluminosilicate NT (see Figure 1 and Figure 6); the average inner diameter increases from 1.4 for the aluminosilicate NT to 2.3 nm for the aluminogermanate NT. In Figure 6, we see that because of the larger diameter of aluminogermanate NT there are five layers of water molecules formed inside the pore and the density fluctuation decreases along the radial direction to the center. As shown in Figure 7, water has almost the same number of hydrogen bonds as bulk

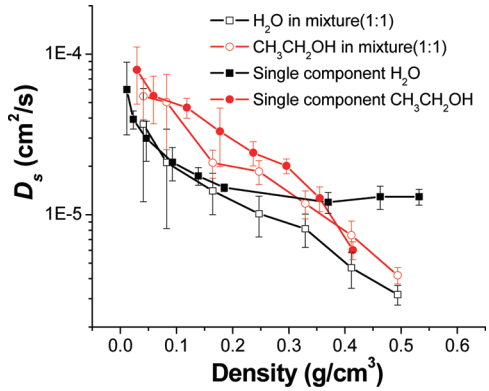

Figure 11. Self-diffusivities of molecules in 1:1 water and ethanol mixtures in the aluminosilicate NT.

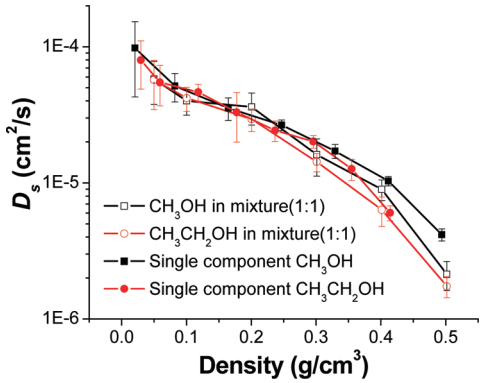

Figure 12. Self-diffusivities of molecules in 1:1 methanol and ethanol mixtures in aluminosilicate NT.

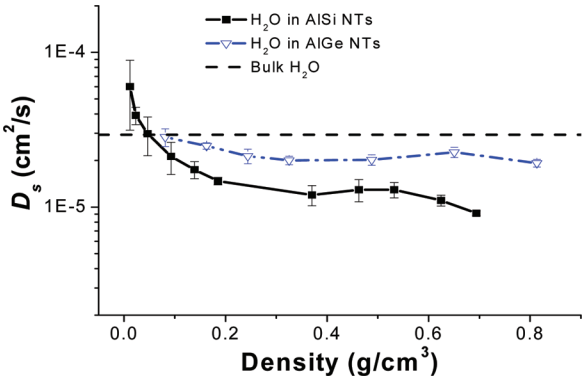

Figure 13. Self-diffusivity of water in aluminosilicate and aluminogermanate NTs. Self-diffusivity of bulk water is shown for comparison.

water when positioned less than 7 Å from tube axis in aluminogermanate NT. For a similar loading of water in the aluminosilicate NT, the region where water is bulk-like is much smaller. At comparable loadings, the ratio of water in this central region to the water in the near wall region is higher in the aluminogermanate than in the aluminosilicate NT. In other words, a larger fraction of water in aluminogermanate NT diffuses as in bulk water.

CONCLUSION

We have studied self-diffusivities of water, methanol, and ethanol and their mixtures in aluminosilicate and aluminogermanate NTs using MD simulations. These NTs are interesting materials because they can be synthesized with monodisperse pore diameters and lengths, a property that is challenging to achieve with nanotubes of other chemical compositions. The diffusivities for all the three single-component liquids in aluminosilicate NT are comparable to the diffusivities observed in bulk liquids. For water, this means that the calculated diffusivities in aluminosilicate NTs are 0−3 orders of magnitude smaller than in carbon NTs, depending on the number of defects in the pore walls of carbon NTs, but considerably larger than in most zeolites. We have shown that the characteristics of diffusion in these materials can be understood by elucidating the nature of hydrogen bonding between molecules in the pore and the pore walls. The primary difference observed between diffusion in aluminosilicate NTs and aluminogermanate NTs is associated with the large pore diameter of the latter materials. The large pore diameter of aluminogermanate NTs allows a large fraction of the molecules in the NT to exist in a bulk-like environment, so the calculated diffusivities in these NTs when they are completely filled with molecules are more similar to the bulk liquids than in the considerably smaller aluminosilicate NTs.

Mixtures of water and methanol in aluminosilicate NTs show a segregation behavior in which water is preferentially located closer to tube wall. The diffusivity of water in these NTs is reduced when alcohol molecules are also present. Qualitatively, this effect is similar to what is seen in the bulk liquid mixtures, but the interplay between molecular interactions and molecule−NT interactions means that the details of the mixture diffusivities in the NT differ quantitatively from the bulk mixtures.

Our calculations have examined molecular diffusion in NTs of infinite extent in the axial direction. An important property of the NTs in current experimental syntheses is that the length of the NTs is monodisperse, with NT lengths in the range of 15−100 nm depending on the Ge content of the materials. In applications of NTs with these dimensions, it is possible that effects due to molecules entering and leaving the pores could play a role in the overall transport properties of molecules through NTs. Although simulation methods have been developed to examine these effects,[32,33] the importance of these effects could only be discussed in a meaningful way if the physical environment in which the NTs would exist in a particular application of interest was defined.

COMPUTATIONAL DETAILS

The details of how structural models were constructed and optimized were described previously by Konduri *et al.*[18] Analogous to their work, we employed the CLAYFF force field[34] to describe the interactions between the atoms in the aluminosilicate NTs. Our calculations for the Ge-containing NT used the interatomic potentials introduced by Konduri *et al.*[9] After relaxation, the outer diameter of the aluminosilicate (germanate) NT is 2.3 (3.4) nm and the unit cell length along the tube axis is 0.84 (0.86) nm, which agree well with experimental measurements.[7]

The simple point charge (SPC) model was used for water. Force field parameters for the NT and water have been described earlier.[9,18] To simulate methanol and ethanol, we used parameters from the TraPPE force field,[35] which accurately describes the vapor−liquid coexistence curves for primary, secondary, and tertiary alcohols. To describe interactions between alcohol molecules, water, and the NTs, the Lorentz−Berthelot combination rules were used for unlike LJ interactions. An Ewald summation was used for Coulombic interactions.

All the MD simulations presented here were performed using the DL_POLY Molecular Simulation Package.[36] In our simula-

tions, periodic boundary conditions were used so that the NTs were hexagonally packed as in earlier simulations,[37] similar to the experimentally observed monoclinic packing.[7] Two unit cells of aluminosilicate and aluminogermanate NTs with 672 and 1008 atoms, respectively, were simulated with periodic boundary condition along the axial direction. To create initial configurations of molecules in the NT pores, molecules were inserted at random positions with the simple rule that insertion was accepted if the total energy of the structure was lowered by the presence of the newly inserted molecule. The configurations created in this way were subjected to energy minimization before MD simulations were performed. We did not consider molecules in the interstitial spaces between NTs because previous Monte Carlo simulations showed that water molecules preferentially adsorb into the pores of the NTs.[18] For each system considered here, NVT-MD simulations at 298 K were performed using a Nosé−Hoover thermostat. After equilibrating the system for 0.4 ns, MD simulations were run for 8 ns. All MD simulations used a time step of 1 fs. Axial self-diffusivities, D_s, were calculated by averaging data over five independent 1.6 ns segments of the overall trajectories. D_s was derived from the mean square displacements (MSD) of the oxygen atom of molecules in the NT *via* the Einstein relation $\langle r^2(t)\rangle = 2D_s t$, where $r(t)$ is the oxygen axial displacement after time t. The radial distribution of molecules, density profiles, and other static properties were obtained by averaging over data taken from configurations separated by 0.4 ps intervals from each trajectory.

Acknowledgment. S.N. acknowledges financial support from the ACS Petroleum Research Fund (#44074-G10) and NSF-CBET (#0403574).

Supporting Information Available: Comparison of calculated self-diffusivities of water and methanol mixtures with 3:1, 1:1, and 1:3 molar ratios in an aluminosilicate NT at 298 K. This material is available free of charge *via* the Internet at http://pubs.acs.org.

REFERENCES AND NOTES

1. Ackerman, W. C.; Smith, D. M.; Huling, J. C.; Kim, Y. W.; Bailey, J. K.; Brinker, C. J. Gas Vapor Adsorption in Imogolite: A Microporous Tubular Aluminosilicate. *Langmuir* **1993**, *9*, 1051–1057.
2. Imamura, S.; Kokubu, T.; Yamashita, T.; Okamoto, Y.; Kajiwara, K.; Kanai, H. Shape-Selective Copper-Loaded Imogolite Catalyst. *J. Catal.* **1996**, *160*, 137–139.
3. Marzan, L. L.; Philipse, A. P. Synthesis of Platinum Nanoparticles in Aqueous Host Dispersions of Inorganic (Imogolite) Rods. *Colloids Surf., A* **1994**, *90*, 95–109.
4. Ohashi, F.; Tomura, S.; Akaku, K.; Hayashi, S.; Wada, S. I. Characterization of Synthetic Imogolite Nanotubes as Gas Storage. *J. Mater. Sci.* **2004**, *39*, 1799–1801.
5. Pohl, P. I.; Faulon, J. L.; Smith, D. M. Pore Structure of Imogolite Computer Models. *Langmuir* **1996**, *12*, 4463–4468.
6. Yamamoto, K.; Otsuka, H.; Takahara, A. Preparation of Novel Polymer Hybrids from Imogolite Nanofiber. *Polym. J.* **2007**, *39*, 1–15.
7. Mukherjee, S.; Bartlow, V. A.; Nair, S. Phenomenology of the Growth of Single-Walled Aluminosilicate and Aluminogermanate Nanotubes of Precise Dimensions. *Chem. Mater.* **2005**, *17*, 4900–4909.
8. Mukherjee, S.; Kim, K.; Nair, S. Short, Highly Ordered, Single-Walled Mixed-Oxide Nanotubes Assemble from Amorphous Nanoparticles. *J. Am. Chem. Soc.* **2007**, *129*, 6820–6826.
9. Konduri, S.; Mukherjee, S.; Nair, S. Controlling Nanotube Dimensions: Correlation between Composition, Diameter, and Internal Energy of Single-Walled Mixed Oxide Nanotubes. *ACS Nano* **2007**, *1*, 393–402.
10. Hinds, B. J.; Chopra, N.; Rantell, T.; Andrews, R.; Gavalas, V.; Bachas, L. G. Aligned Multiwalled Carbon Nanotube Membranes. *Science* **2004**, *303*, 62–65.
11. Holt, J. K.; Park, H. G.; Wang, Y. M.; Stadermann, M.; Artyukhin, A. B.; Grigoropoulos, C. P.; Noy, A.; Bakajin, O. Fast Mass Transport through Sub-2-Nanometer Carbon Nanotubes. *Science* **2006**, *312*, 1034–1037.
12. Hummer, G.; Rasaiah, J. C.; Noworyta, J. P. Water Conduction through the Hydrophobic Channel of a Carbon Nanotube. *Nature* **2001**, *414*, 188–190.
13. Kalra, A.; Garde, S.; Hummer, G. Osmotic Water Transport through Carbon Nanotube Membranes. *Proc. Natl. Acad. Sci. U.S.A.* **2003**, *100*, 10175–10180.
14. Majumder, M.; Chopra, N.; Andrews, R.; Hinds, B. J. Nanoscale Hydrodynamics: Enhanced Flow in Carbon Nanotubes. *Nature* **2005**, *438*, 44.
15. Noy, A.; Park, H. G.; Fornasiero, F.; Holt, J. K.; Grigoropoulos, C. P.; Bakajin, O. Nanofluidics in Carbon Nanotubes. *Nano Today* **2007**, *2*, 22–29.
16. Skoulidas, A. I.; Ackerman, D. M.; Johnson, J. K.; Sholl, D. S. Rapid Transport of Gases in Carbon Nanotubes. *Phys. Rev. Lett.* **2002**, *89*, 185901–185904.
17. Verweij, H.; Schillo, M. C.; Li, J. Fast Mass Transport through Carbon Nanotube Membranes. *Small* **2007**, *3*, 1996–2004.
18. Konduri, S.; Tong, H. M.; Chempath, S.; Nair, S. Water in Single-Walled Aluminosilicate Nanotubes: Diffusion and Adsorption Properties. *J. Phys. Chem. C* **2008**, *112*, 15367–15374.
19. Guimaraes, L.; Enyashin, A. N.; Frenzel, J.; Heine, T.; Duarte, H. A.; Seifert, G. Imogolite Nanotubes: Stability, Electronic, and Mechanical Properties. *ACS Nano* **2007**, *1*, 362–368.
20. Konduri, S.; Mukherjee, S.; Nair, S. Strain Energy Minimum and Vibrational Properties of Single-Walled Aluminosilicate Nanotubes. *Phys. Rev. B* **2006**, *74*, 033401–033404.
21. Jeffrey, G. A. *An Introduction to Hydrogen Bonding*; Oxford University Press: New York, 1997; p vii.
22. Sholl, D. S.; Skodje, R. T. Diffusion of Xenon on a Platinum Surface: The Influence of Correlated Flights. *Physica D* **1994**, *71*, 168–184.
23. Sholl, D. S.; Fichthorn, K. A. Effect of Correlated Flights on Particle Mobilities during Single-File Diffusion. *Phys. Rev. E* **1997**, *55*, 7753–7756.
24. Gordillo, M. C.; Marti, J. Hydrogen Bond Structure of Liquid Water Confined in Nanotubes. *Chem. Phys. Lett.* **2000**, *329*, 341–345.
25. Striolo, A. The Mechanism of Water Diffusion in Narrow Carbon Nanotubes. *Nano Lett.* **2006**, *6*, 633–639.
26. Liu, Y. C.; Shen, J. W.; Gubbins, K. E.; Moore, J. D.; Wu, T.; Wang, Q. Diffusion Dynamics of Water Controlled by Topology of Potential Energy Surface Inside Carbon Nanotubes. *Phys. Rev. B* **2008**, *77*, 125438-7.
27. Mamontov, E.; Burnham, C. J.; Chen, S. H.; Moravsky, A. P.; Loong, C. K.; de Souza, N. R.; Kolesnikov, A. I. Dynamics of Water Confined in Single- and Double-Wall Carbon Nanotubes. *J. Chem. Phys.* **2006**, *124*, 194703–194706.
28. Won, C. Y.; Joseph, S.; Aluru, N. R. Effect of Quantum Partial Charges on the Structure and Dynamics of Water in Single-Walled Carbon Nanotubes. *J. Chem. Phys.* **2006**, *125*, 114701–114709.
29. Striolo, A. Water Self-Diffusion through Narrow Oxygenated Carbon Nanotubes. *Nanotechnology* **2007**, *18*, 475704–475710.
30. Won, C. Y.; Aluru, N. R. Water Permeation through a Subnanometer Boron Nitride Nanotube. *J. Am. Chem. Soc.* **2007**, *129*, 2748–2749.
31. Paoli, H.; Methivier, A.; Jobic, H.; Krause, C.; Pfeifer, H.; Stallmach, F.; Karger, J. Comparative QENS and PFG NMR Diffusion Studies of Water in Zeolite NaCaA. *Microporous Mesoporous Mater.* **2002**, *55*, 147–158.
32. Newsome, D. A.; Sholl, D. S. Predictive Assessment of Surface Resistances in Zeolite Membranes Using Atomically Detailed Models. *J. Phys. Chem. B* **2005**, *109*, 7237–7244.
33. Newsome, D. A.; Sholl, D. S. Influences of Interfacial Resistances on Gas Transport through Carbon Nanotube Membranes. *Nano Lett.* **2006**, *6*, 2150–2153.
34. Cygan, R. T.; Liang, J. J.; Kalinichev, A. G. Molecular Models of Hydroxide, Oxyhydroxide, and Clay Phases and the Development of a General Force Field. *J. Phys. Chem. B* **2004**, *108*, 1255–1266.

35. Chen, B.; Potoff, J. J.; Siepmann, J. I. Monte Carlo Calculations for Alcohols and Their Mixtures with Alkanes. Transferable Potentials for Phase Equilibria. 5. United-Atom Description of Primary, Secondary, And Tertiary Alcohols. *J. Phys. Chem. B* **2001**, *105*, 3093–3104.
36. http://www.cse.scitech.ac.uk/ccg/software/DL_POLY/. DL_POLY is a package of molecular simulation routines: Smith, W.; Forester, T. R.; *DL_POLY*; The Council for the Central Laboratory of the Research Councils, Daresbury Laboratory: Daresbury, Warrington, U.K., 1996.
37. Tamura, K.; Kawamura, K. Molecular Dynamics Modeling of Tubular Aluminum Silicate: Imogolite. *J. Phys. Chem. B* **2002**, *106*, 271–278.